Diffraction theory and the double-charge-exchange reaction $^{18}O(\pi^+,\pi^-)^{18}Ne$

L. C. Liu
Los Alamos National Laboratory, Los Alamos, New Mexico 87545
(Received 10 December 1981; revised manuscript received 25 October 1982)

The angular distribution and the excitation function of the reaction $^{18}O(\pi^+,\pi^-)^{18}Ne$ (double isobaric analog state) can be well understood in the framework of a coupled-channel diffractive scattering theory provided we include higher-order processes. Use of a scaling theory allows an essentially parameter-free calculation of these processes and makes possible the study of effects arising from finer aspects of nuclear structure such as the core excitation of ^{18}O.

NUCLEAR REACTIONS $^{18}O(\pi^+,\pi^-)^{18}Ne$ (DIAS) at $T_\pi=50$–300 MeV; excitation functions; elastic and double-charge-exchange differential cross sections; effects of two-nucleon processes and nuclear structure.

I. INTRODUCTION

Pion-nucleus double-charge-exchange (DCE) reactions are of special interest in that the leading dynamical process involves the scattering of the pion by two nucleons. An understanding of pion DCE reactions may therefore give us new information about the two-nucleon aspect of nuclear dynamics. Several pion DCE experiments leading to double isobaric analog states (DIAS) have been performed at the Clinton P. Anderson Meson Physics Facility (LAMPF).[1–3] In the case of $^{18}O(\pi^+,\pi^-)^{18}Ne$ (DIAS), differential cross sections were measured between 5° and 40° for pion energies of 164 and 292 MeV. Since the initial and final nuclei are analogs, this DCE process is a coherent one and should be well explained by diffractive scattering theories. The simplest consequence is that the first minimum in the angular distribution, θ_{min}, should normally occur at a smaller angle for higher incident pion energy. But inspection of the data in Figs. 1(a) and (b) shows just the opposite, well outside of experimental error. This paradox has puzzled many researchers. For $T_\pi=164$ MeV, the experimental θ_{min} is found to be at $\sim 20°$. However, nearly all published calculations using a realistic size for ^{18}O give $\theta_{min}\simeq 30°$–40°, quite independent of whether the calculation is made with only the analog intermediate state[4] or with the inclusion of nonanalog intermediate states.[5,6] Oset *et al.*[7] examined nuclear structure effects by using *sd*-shell configuration mixing for the valence neutrons while assuming an inert ^{16}O core. They found that θ_{min} was insensitive to the various admixtures used. One may ask, therefore, is the DCE reaction diffractive? In this work we show that the DCE data can be accounted for by diffractive scattering theory, provided the reaction mechanism and the nuclear structure are treated properly.

In the next section, we develop the basic theory for DCE reactions leading to DIAS. We introduce into our theory a generalized second-order pion-nucleus interaction. By the construction of model space, the diagonal matrix elements of this interaction are the second-order pion-nucleus optical potentials in the corresponding elastic channels, while the off-diagonal elements are irreducible two-nucleon processes involving pion single-charge exchanges (SCE) and double-charge exchanges. From the analytic structure of the theory, we see that these two-nucleon processes, interfering with the conventional sequential one-nucleon-SCE processes which involve only valence nucleons, can have important effects on calculated DCE cross sections. Owing to the lack of systematic pion-^{18}O elastic scattering data at pion energies between 50 and 300 MeV, we use an isospin scaling model to construct the second-order pion-nucleus interaction for π^+-^{18}O and its analog systems from a knowledge of the previously determined pion-^{16}O second-order optical potentials. The basic dynamical assumption in the scaling model is that true pion absorption represents the dominant two-nucleon reaction mechanism across the (3,3) resonance region. Theoretical results are given in Sec. III. We see that our theory gives a satisfactory description of both the 5°-excitation function and the angular distributions of the DCE reaction $^{18}O(\pi^+,\pi^-)^{18}Ne$ (DIAS) at various energies. Our

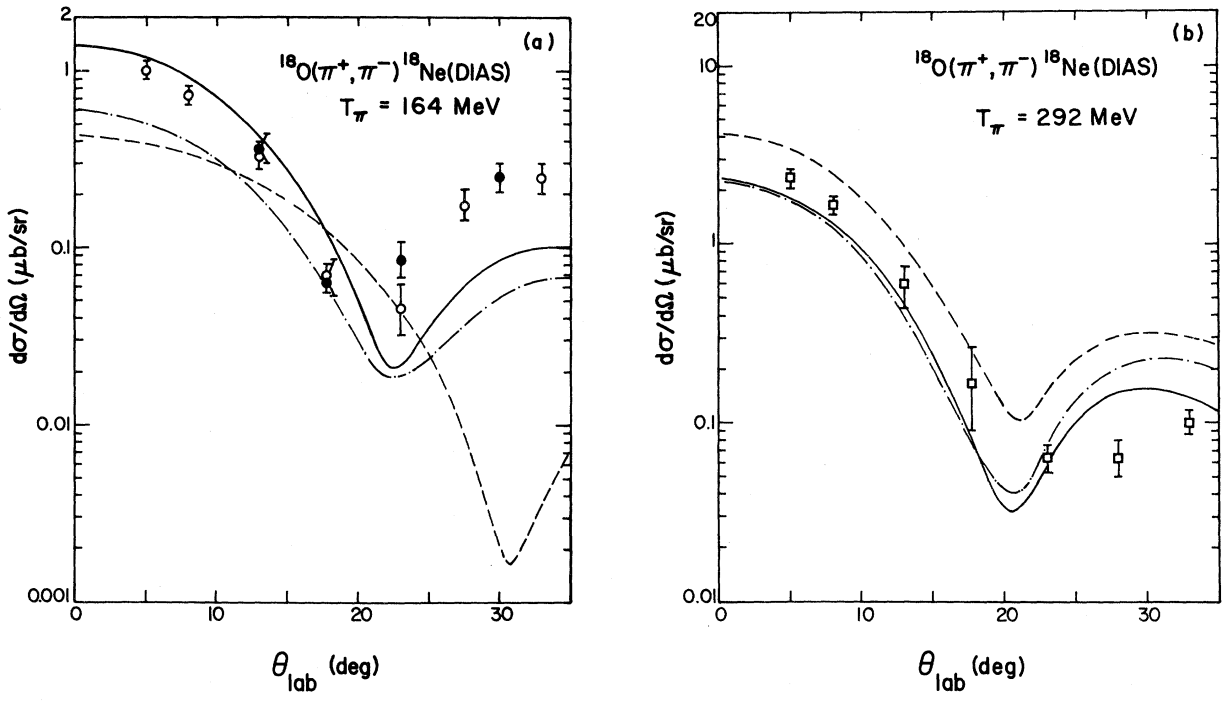

FIG. 1. (a) Angular distributions of the reaction $^{18}O(\pi^+,\pi^-)^{18}Ne$ (DIAS) at 164 MeV. Data are from Ref. 1 (●) and Ref. 3 (○). The data of Ref. 1 were transformed into the laboratory system. The dashed curve represents theoretical results obtained without the inclusion of the ρ^2-dependent interaction. Results obtained with the inclusion of the ρ^2-dependent interaction based on true pion absorption alone are shown, respectively, as the dotted-dashed curve when the inert-core nuclear model is used, and as the solid curve when the core excitation model is used. (b) Angular distributions of the reaction $^{18}O(\pi^+,\pi^-)^{18}Ne$ (DIAS) at 292 MeV. Data are from Ref. 3 (□). Notation for curves is the same as for Fig. 1(a).

theory is equally able to describe the available π^+-^{18}O elastic scattering differential cross section data. It is noteworthy that no adjustable parameter was used in these calculations. We also discuss, in particular, effects arising from the inclusion of the two-nucleon reaction mechanism and from nuclear structure details such as the core excitation in ^{18}O. Finally, we summarize our findings in Sec. IV.

II. BASIC THEORY

We use a momentum-space coupled-channel formalism.[8] For this study, we define a model space containing three elastic channels: (a) π^+-^{18}O (g.s.); (b) π^0-^{18}F (IAS); (c) π^--^{18}Ne (DIAS). Formal elimination of other channels leads to three coupled integral equations of the form

$$\mathcal{T}=\tilde{\mathcal{V}}+\tilde{\mathcal{V}}G^{0(+)}\mathcal{T}\ , \tag{1}$$

where $\mathcal{T}$ and $\tilde{\mathcal{V}}$ are, respectively, the scattering operator and an effective interaction. We decompose $\tilde{\mathcal{V}}$ into its strong and Coulomb interaction components, $\tilde{\mathcal{V}}=V_s+V_c$. In the model space, the isospin-conserving V_s is complex and energy-dependent, while V_c is real and breaks the isospin symmetry. We can identify the diagonal matrix elements of V_s with the π-nucleus optical potentials in the corresponding elastic channels.[8] The off-diagonal matrix elements of V_s are the various SCE and DCE interactions coupling the elastic channels. Once the interaction $\tilde{\mathcal{V}}$ is determined, we solve the coupled equations with appropriate boundary conditions to obtain the elastic and charge-exchange cross sections.

For nuclei with isospin $T\geq 1$, the strong interaction has the general form

$$V_s=V_0+(\vec{I}\cdot\vec{T})V_1+(\vec{I}\cdot\vec{T})^2V_2$$

in the isospin space. Here $\vec{I}$ and $\vec{T}$ are, respectively, the pion and nuclear isospin operator. In the literature, V_0, V_1, and V_2 are, respectively, referred to as the isoscalar, isovector, and isotensor interactions. For the Coulomb interaction, we use the expression

$$V_c=I_3Z_iu_c-(T-2+T_3)(T+T_3)\Delta_b$$
$$+(T+T_3)(T-1+T_3)\Delta_c/2\ ,$$

where I_3 and T_3 are the third component of $\vec{I}$ and $\vec{T}$. Z is the nuclear charge operator having the property $Z\,|\,i\rangle = z_i\,|\,i\rangle$, where z_i is the nuclear charge in the channel i. We have $z_a = 8$, $z_b = 9$, and $z_c = 10$. The u_c is a unit Coulomb potential taken to be the potential between a π^+ and a positive charge distributed uniformly on a sphere of radius R_c. We take $R_c = 3.6$ fm. The quantities Δ_b and Δ_c denote, respectively, the mass differences, corrected for the excitation energy of channels b and c with respect to channel a. In the present case $\Delta_b = -1.92$ MeV and $\Delta_c = 6.1$ MeV. It is easy to show that in the isospin space the matrix elements of the full interaction $\tilde{\mathscr{V}}$ are given by:

$$\tilde{\mathscr{V}}_{aa} = V_0 - V_1 + 2V_2 + 8u_c \ ,$$

$$\tilde{\mathscr{V}}_{bb} = V_0 + 2V_2 + \Delta_b \ ,$$

$$\tilde{\mathscr{V}}_{cc} = V_0 - V_1 + 2V_2 - 10u_c + \Delta_c \ ,$$

$$\tilde{\mathscr{V}}_{ab} = \tilde{\mathscr{V}}_{ba} = V_1 - V_2 \ ,$$

$$\tilde{\mathscr{V}}_{bc} = \tilde{\mathscr{V}}_{cb} = V_1 - V_2 \ ,$$

and

$$\tilde{\mathscr{V}}_{ac} = \tilde{\mathscr{V}}_{ca} = V_2 \ .$$

We now proceed to show how the quantities V_0, V_1, and V_2, and whence the full interaction $\tilde{\mathscr{V}}$, can be determined from a knowledge of the pion-nucleus optical potentials. We introduce the optical potentials for the π^i-^{18}O systems ($i = +,0,-$) by using the relations

$$V_{\text{opt},i} = \langle \pi^i, {}^{18}\text{O(g.s.)}\,|\,V_s\,|\,\pi^i, {}^{18}\text{O(g.s.)}\rangle \ .$$

Standard angular momentum algebra calculations lead to the simple result

$$\begin{bmatrix} V_0 \\ V_1 \\ V_2 \end{bmatrix} = \frac{1}{T(2T-1)} \begin{bmatrix} -T & T(2T+1) & -T \\ 1-T & -1 & T \\ 1 & -2 & 1 \end{bmatrix} \begin{bmatrix} V_{\text{opt},+} \\ V_{\text{opt},0} \\ V_{\text{opt},-} \end{bmatrix} , \tag{2}$$

where T is the nuclear isospin. ($T = 1$ for ^{18}O.) It is useful to expand both sides of Eq. (2) by defining

$$V_{\text{opt},i} = \sum_n V^{(n)}_{\text{opt},i} \quad (i = +,0,-)$$

and

$$V_j = \sum_n V^{(n)}_j \quad (j = 0,1,2) \ .$$

Here $V^{(n)}_{\text{opt},i}$ denotes the nth order π^i-^{18}O optical potential. The linearity of Eq. (2) suggests that the relations between V_0, V_1, V_2, and the optical potentials hold at each order of the expansion. We emphasize that for optical potentials we are using an expansion in the number of target nucleons that interact with the projectile.[9] The second-order optical potential refers, therefore, to that part of the optical potential which involves the pion interaction with two nucleons and which cannot be reduced to one-nucleon processes.

Although we solve the coupled integral equations to all orders, we can gain insight into the DCE reaction by examining the leading terms in the iteration of Eq. (1). We write, therefore, the DCE amplitude in the form

$$\mathscr{T}_{ac} = \tilde{\mathscr{V}}_{ac} + \tilde{\mathscr{V}}_{aa} G_a^{0(+)} \tilde{\mathscr{V}}_{ac} + \tilde{\mathscr{V}}_{ab} G_b^{0(+)} \tilde{\mathscr{V}}_{bc} + \tilde{\mathscr{V}}_{ac} G_c^{0(+)} \tilde{\mathscr{V}}_{cc} + \cdots \ . \tag{3}$$

One can show[10] that

$$\tilde{\mathscr{V}}^{(1)}_{ac} (\equiv \tilde{\mathscr{V}}^{(1)}_{ca} = V^{(1)}_2) = 0$$

for $V^{(1)}_{\text{opt},i}$ that are proportional to $t\rho$ where t is the πN scattering amplitude and ρ the nuclear density. Consequently, when only the $V^{(1)}_{\text{opt},i}$ are present in the theory, the leading contribution to the DCE reaction comes from $\tilde{\mathscr{V}}^{(1)}_{ab} G_b^{0(+)} \tilde{\mathscr{V}}^{(1)}_{bc}$ or two sequential one-nucleon SCE processes via the analog channel b. However, analyses of π-nucleus elastic scattering[11,12] have shown the importance of second-order optical potentials. The $V^{(2)}_{\text{opt},i}$ will lead to $V^{(2)}_0$, $V^{(2)}_1$, and $V^{(2)}_2$ which are, in general, not equal to zero. Thus, when two-nucleon processes are included in the dynamical calculation,

$$\tilde{\mathscr{V}}_{ac} = \tilde{\mathscr{V}}^{(2)}_{ac} = V^{(2)}_2 \neq 0 \ .$$

Consequently,

$$\begin{aligned} \mathscr{T}_{ac} = \{ & \tilde{\mathscr{V}}^{(2)}_{ac} + \tilde{\mathscr{V}}^{(1;2)}_{aa} G_a^{0(+)} \tilde{\mathscr{V}}^{(2)}_{ac} \\ & + \tilde{\mathscr{V}}^{(2)}_{ac} G_c^{0(+)} \tilde{\mathscr{V}}^{(1;2)}_{cc} + \tilde{\mathscr{V}}^{(1)}_{ab} G_b^{0(+)} \tilde{\mathscr{V}}^{(2)}_{bc} \\ & + \tilde{\mathscr{V}}^{(2)}_{ab} G_b^{0(+)} \tilde{\mathscr{V}}^{(1)}_{bc} + \tilde{\mathscr{V}}^{(2)}_{ab} G_b^{0(+)} \tilde{\mathscr{V}}^{(2)}_{bc} \} \\ & + \tilde{\mathscr{V}}^{(1)}_{ab} G_b^{0(+)} \tilde{\mathscr{V}}^{(1)}_{bc} + \cdots \ , \end{aligned} \tag{4}$$

where

$$\tilde{\mathscr{V}}^{(1;2)}_{ij} \equiv \tilde{\mathscr{V}}^{(1)}_{ij} + \tilde{\mathscr{V}}^{(2)}_{ij} \quad (i,j = a,b,c) \ .$$

The sum of the amplitudes inside the curly brackets can be of strength comparable to $\tilde{\mathscr{V}}^{(1)}_{ab} G_b^{0(+)} \tilde{\mathscr{V}}^{(1)}_{bc}$. By construction, $\tilde{\mathscr{V}}^{(2)}_{ac}$ represents the DCE processes on two valence nucleons via nonanalog intermediate

states. On the other hand, $\tilde{\mathscr{V}}_{ab}^{(2)}$ and $\tilde{\mathscr{V}}_{bc}^{(2)}$ are the two-nucleon SCE processes involving nonanalog intermediate states in which valence as well as core nucleons participate. The discussion above shows the connection between pion charge exchanges on core nucleons and the pion-nucleus second-order optical potential. Conversely, the observed importance of the second-order optical potential in the analysis of elastic scattering is a strong indication that any realistic DCE theory must take into account pion charge exchanges on *core* nucleons.

As we can see from Eq. (2), a complete knowledge of the set of potentials $V_{\mathrm{opt},i}$ $(i=+,0,-)$ leads to a unique set of values for V_0, V_1, and V_2, and, hence, to a definite prediction of the DCE cross sections. Accordingly, we start our analysis with the determination of the $V_{\mathrm{opt},i}$. Our approach differs from the more commonly used one in which the ρ^2-dependent $V_0^{(2)}$, $V_1^{(2)}$, and $V_2^{(2)}$ are treated as three complex quantities, determined by fitting simultaneously the elastic and charge-exchange differential cross sections. Clearly this latter approach can no longer be used to predict DCE reactions, and it obscures nuclear structure effects. In the present study, we calculate the $V_{\mathrm{opt},i}^{(1)}$ using a microscopic theory[12] and determine the $V_{\mathrm{opt},i}^{(2)}$ from a knowledge of the π-^{16}O second-order optical potential[12] by means of an isospin scaling model.[8] (The need of a scaling model is due solely to the lack of systematic experimental information on π-^{18}O elastic scattering.) A brief description of the scaling model is in order.

In most studies the phenomenological momentum-space pion-nucleus second-order optical potential has been expressed in the form

$$V_{\mathrm{opt}}^{(2)}(E;\vec{k}',\vec{k})=KM(E,\theta)\sum_{\alpha,\beta\neq\alpha}\rho_{\alpha\beta}^{2}(\vec{q})\ ,$$

where K is a kinematic factor and E, θ, and $\vec{q}$ are the energy of the system, the pion scattering angle, and the momentum transfer, respectively. The nuclear structure information is contained in the form factor $\rho_{\alpha\beta}^{2}(\vec{q})$, which is the Fourier transform of the product $\rho_\alpha(\vec{r})\rho_\beta(\vec{r})$ of the single-nucleon density distributions of the nucleons α and β. The function $M(E,\theta)$ has the meaning of an *average* interaction strength between the pion and a nucleon pair. A standard parametrization[11] is

$$M(E,\theta)=B(E)+\vec{k}'\cdot\vec{k}C(E)\ ,$$

where B and C are complex quantities determined from a fit to elastic scattering data. For ^{18}O, we separate the second-order potential into three terms:

$$V_{\mathrm{opt},i}^{(2)}(E;\vec{k}',\vec{k})=K\left[M_{i,cc}(E,\theta)\sum_{\alpha_c,\beta_c\neq\alpha_c}\rho_{\alpha_c\beta_c}{}^{2}(\vec{q})+M_{i,vc}(E,\theta)\sum_{\alpha_c,\beta_v}\rho_{\alpha_c\beta_v}{}^{2}(\vec{q})+M_{i,vv}(E,\theta)\sum_{\alpha_v,\beta_v\neq\alpha_v}\rho_{\alpha_v\beta_v}{}^{2}(\vec{q})\right]\ , \tag{5}$$

where i $(=+,0,-)$ denotes the pion charge state. We have used the subscripts v and c to label the valences and core nucleons. For example, $M_{i,vc}$ represents the interaction strength between π^i and a valence-core nucleon pair averaged over all possible isospin states associated with the pair. In our scaling model we take $M_{i,cc}$ to be given by the M function of π-^{16}O scattering, and assume that

$$M_{i,vc}\equiv\eta_{i,vc}(E)M_{i,cc}(E,\theta)$$

and

$$M_{i,vv}\equiv\eta_{i,vv}(E)M_{i,cc}(E,\theta)\ .$$

Here the η_i are the scaling factors. Using the notation of Ref. 8, we can write

$$\eta_{i,vc}(E)\equiv\bar{S}(\pi^i(n_vN_c))/\bar{S}(\pi(N_cN_c))$$

and

$$\eta_{i,vv}(E)\equiv S(\pi^i(nn))/\bar{S}(\pi(N_cN_c))\ .$$

The $\bar{S}$ and S are the energy-dependent strength functions in isospin space. They are functionals of elementary pion-nucleon amplitudes, and can be determined once a specific reaction mechanism is defined. We refer to Appendix A for detailed discussion and notation. We can see that the use of the scaling method is facilitated by the separation of the nuclear form factor from the interaction strength in the parametrization of the second-order pion-nucleus optical potential. We emphasize that the scaling method allows us to obtain the second-order optical potentials for π^i-^{18}O systems $(i=+,0,-)$ from a knowledge of the second-order pion-^{16}O optical potential, and thus, through the use of Eq. (2), the ρ^2-dependent isoscalar, isovector, and isotensor components of the pion-nucleus interaction.

We have noted[8] that two different reaction mechanisms can contribute to the ρ^2 term of the pion-nucleus potential, namely, the absorption and reemission of a pion by a pair of nucleons, and the scattering of the pion by two short-range-correlated nucleons. Thus, more generally, we have

$$\eta_i(E)=[1-X(E)]\eta_i^A(E)+X(E)\eta_i^B(E) .$$

Here η_i^A and η_i^B are, respectively, the scaling factors calculated according to true pion absorption and short-range correlations processes. The quantity $X(E)$ $[0\leq X(E)\leq 1]$ takes into account the relative importance of these two reaction mechanisms. Consequently, when only the true pion absorption contributes, we have, by definition, $X=0$. The analysis of electron scattering data and the study of high-energy pion-nucleus elastic scattering indicate that short-range correlation effects may become important only at momentum transfer $q>2.5$ fm^{-1} (Ref. 13). Since this large q value cannot be reached in pion scattering from ^{16}O at pion energies below 180 MeV, we can assume that contributions to the phenomenological pion-^{16}O second-order optical potential at $T_\pi \leq 180$ MeV arise from true pion absorption alone, i.e., $X=0$. The value of X at higher energies cannot be set unambiguously, since the reported quantitative effects of short-range correlations on calculated electron-nucleus and hadron-nucleus elastic scattering cross sections are strongly model dependent. We therefore use $X=0$ at all energies in our calculations and look for qualitative evidence for short-range correlations by comparing theoretical calculations based on true pion absorption alone with the experimental DCE *differential* cross sections at 292 MeV.

In addition to the usual inert-core approximation, we have examined nuclear structure effects by assuming that ^{16}O core is *not* inert. We use a coexistence model and write[14]:

$$|\,^{18}\mathrm{O(g.s.)}\rangle = a\,|(1d^{\nu}_{5/2})_{J=0}{}^2\rangle + b\,|(2s^{\nu}_{1/2})_{J=0}{}^2\rangle + c\,|\Psi_{00}\rangle . \quad (6)$$

where Ψ_{00} is a collective state containing the excitation of core protons. Again, for the purpose of testing our reaction theory and the scaling model, we do not vary the coefficients in Eq. (6) and we use the wave function determined in Ref. 14, which corresponds to $a=0.842$, $b=0.440$, and $c=-0.313$. We have used harmonic oscillator wave functions for $(1d^{\nu}_{5/2})^2$ and $(2s^{\nu}_{1/2})^2$ and as the spherical basis for expanding the intrinsic deformed wave functions in the coexistence model. For the other nucleons, we used the DME Hartree-Fock (HF) wave function.[15] The harmonic oscillator parameter was chosen to give for ^{18}O a root mean square (rms) radius $r_n=2.85$ fm for the neutron distribution.[16] Both the $V^{(1)}_{\mathrm{opt},i}$ and $V^{(2)}_{\mathrm{opt},i}$ were calculated with these wave functions. When the inert-core assumption was used, we employed DME HF wave functions for all the nucleons.

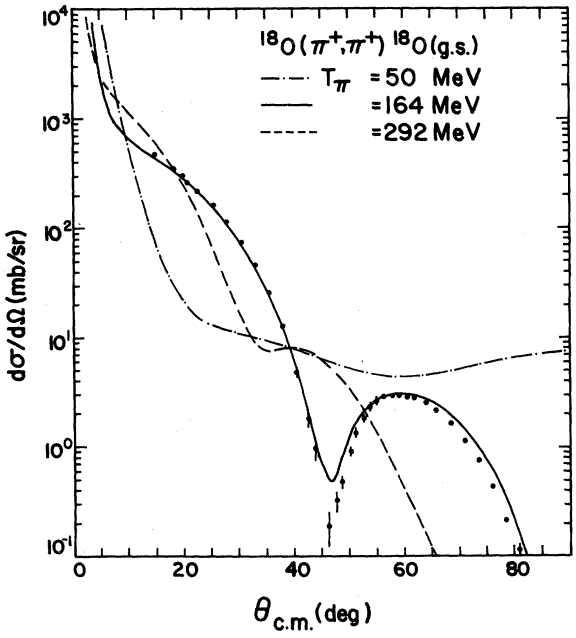

FIG. 2. The π^+-^{18}O elastic differential cross sections at 50, 164, and 292 MeV. Data at 164 MeV are from Ref. 17. Theoretical curves are obtained with the inclusion of the ρ^2-dependent interaction based on true pion absorption and the inert-core nuclear model.

III. RESULTS AND DISCUSSION

The π^+-^{18}O elastic cross sections predicted by the scaling model based on the true pion absorption mechanism and the inert-core nuclear model are shown in Fig. 2 for pion energies 50, 164, and 292 MeV. Inclusion of core excitations gives very similar elastic cross sections that cannot be distinguished from the curves of Fig. 2. The second-order pion-^{16}O optical potential parameters were obtained from a smooth interpolation between the values determined in Ref. 12. The interpolation procedure is outlined in Appendix B. It is of interest to check whether the parameters determined by interpolation are reasonable. For this purpose, we further compare the theoretical cross sections with experimental π^+-^{18}O elastic scattering cross sections at 230 MeV (Fig. 3). Here, the solid curve represents the theoretical cross sections calculated with the same assumptions of reaction mechanism and nuclear model as those used in obtaining the curves of Fig. 2. Again, theoretical results corresponding to the inclusion of core excitation are not shown, since they are very similar to the ones represented by the solid curve. Although the calculated elastic cross sections are insensitive to this finer aspect of the nuclear structure

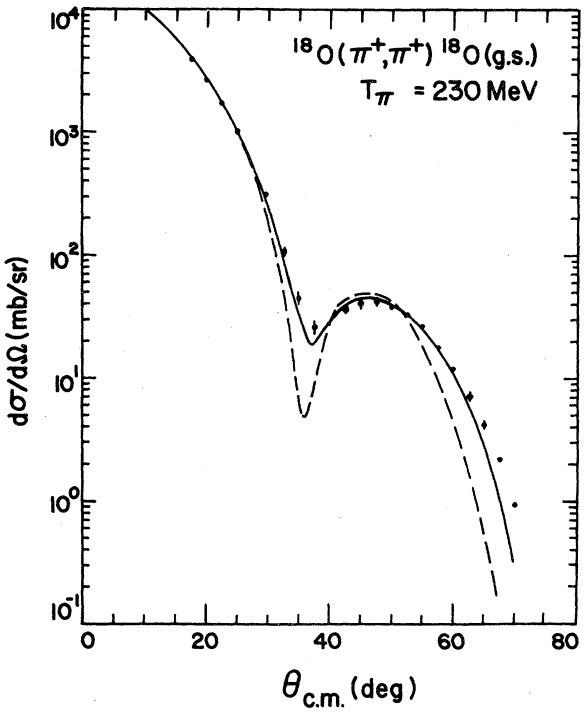

FIG. 3. The π^+-^{18}O elastic differential cross sections at 230 MeV. Data are from Ref. 18. Notation for curves is the same as for Fig. 1.

model used, they do depend appreciably on whether or not the $V^{(2)}_{\text{opt},i}$ are included in the theory. To illustrate this dependence, we also present in Fig. 3 theoretical cross sections calculated with $V^{(1)}_{\text{opt},i}$ (dashed curve). The good agreement of available data[17,18] at 164 and 230 MeV with the calculations based on the scaling model provides some support for the latter. It would be of interest to see if our predictions could be confirmed by measurements at other energies.

In Fig. 1(a) we have represented the inert-core model DCE cross sections obtained with and without the ρ^2 term by dotted-dashed and dashed curves. The most remarkable effect of the ρ^2 term is to move the $\theta_{\min}$ at 164 MeV from $\sim 30°$ to $\sim 23°$. However, both these curves underestimates the magnitude of the experimental differential cross sections. The coexistence model gives a better result for the forward-angle cross sections. Results obtained with the true pion absorption mechanism and with the nuclear wave function of Ref. 14 are shown as the solid curve. We also found that using the nuclear wave function of Ref. 14 but with the ρ^2-dependent interactions turned off led to a $\theta_{\min}$ very similar to that of the dashed curve. In other words, the use of a nuclear wave function of the form given by Eq. (6) mainly affects the magnitude of DCE cross sections, in agreement with the general findings of Ref. 7 where the various trial nuclear wave functions used correspond to the special case of $c=0$. Thus, we can ascribe the drastic change in the position of $\theta_{\min}$ to the inclusion of the ρ^2-dependent interaction. The calculated DCE angular distributions at 292 MeV are shown in Fig. 1(b). Notation for the curve is the same as that for Fig. 1(a). Again, the theoretical results are improved by the use of the scaling model and a nuclear wave function with core excitation. We also note that the solid curve already gives a reasonable description of the differential cross sections, indicating that there is no compelling need for including ρ^2 terms based on short-range correlations. A comment of the position of $\theta_{\min}$ at 292 MeV is in order. Our theory (the solid curve) predicts a $\theta_{\min} \simeq 20°$, which is not inconsistent with the gross feature of the data. However, we see the importance of experimental errors in the differential cross section near $\theta = 28°$. If improved measurements in this neighborhood still led to $\theta_{\min} \simeq 25°$, then it could be interpreted as evidence for the need of including ρ^2-dependent short-range correlations, which would increase the calculated $\theta_{\min}$. For example, with the inclusion of core excitation and the use of $X=0.5$ (i.e., an equal admixture of true absorption and short-range-correlation contributions to the ρ^2-dependent interaction), we obtain a good fit to the data with $\theta_{\min} \simeq 24°$ and a change of the second maximum of the angular distribution from $\sim 30°$ in Fig. 1(b) to $\sim 34°$. (To avoid crowding in the figure, we present the calculated differential cross sections for $X=0.5$ in Table I.) Comparing Table I and the solid curve in Fig. 1(b), we note that the introduction of short-range correlations has only a weak effect on the magnitude of small-angle differential cross sections. Since, as discussed in Sec. II, the value of X cannot be set unambiguously at pion energies > 180 MeV, we believe a remeasurement of the large-angle differential cross sections at 292 MeV would be of great significance in offering an insight into the role of short-range correlations in pion DCE reactions. In the absence of more detailed data in the vicinity of the cross section minimum, we are reluctant to attach any further significance to the X value derived by this procedure.

Calculated 5° excitation functions are given in Fig. 4. We observe again the important effects due to the ρ^2 term, especially at low energies. The enhancement of the cross section at ~ 140 MeV is due directly to the large $\text{Im}[V^{(2)}_{\text{opt}}]$ of the π-^{16}O system,[12] hence the large $\text{Im}[V^{(2)}_{\text{opt}}]$ of the π-^{18}O system, which indicates that an important portion of the pion flux goes from the elastic channel to the DCE channel. We find that the spin-flip part of the

TABLE I. The differential cross sections of $^{18}O(\pi^+,\pi^-)^{18}Ne$ (DIAS) at 292 MeV, calculated with the inclusion of core excitation and with $X=0.5$.

θ_{lab}	0°	5°	10°	15°	20°	24°	30°	34°	40°
$d\sigma/d\Omega$ (μb/sr)	2.20	1.91	1.09	0.47	0.094	0.053	0.13	0.154	0.104

sequential SCE processes on valence neutrons gives very small contributions. It has no effect on θ_{min} at 164 and 292 MeV and its corrections to the cross sections represented by the dashed curve in Fig. 4 are -2%, -15%, and -8% at pion energies 50, 150, and 200 MeV, respectively, in qualitative agreement with Ref. 19. We have included the s-, p-, d-, and f-wave πN interaction in the calculations. At 292 MeV, inclusion of the πN d and f waves increases the calculated cross sections by $\sim 20\%$ at forward angles. The curves in Figs. 1–4 are obtained with the CERN-TH phase shifts,[20] which give cross sections $\sim 4\%$ lower than those obtained with Rowe, Salomon, and Landau (RSL) phase shifts[20] at $T_\pi = 80$–150 MeV and yield similar results at other energies.

It may be helpful to outline the connection between the theory presented in this work and the two-amplitude parametrization of the pion-^{18}O DCE excitation function used by Greene *et al.*[3] In the latter work, the pion-^{18}O DCE amplitude was parametrized as

$$A(E)+B(E) \equiv a(E)\exp[i\phi_a(E)] + b(E)\exp[i\phi_b(E)] ,$$

where the quantities a, b, ϕ_a, and ϕ_b depend on the pion energy E. The first term represents the pion-^{16}O-core DCE amplitude and the second term represents the amplitude corresponding to pion DCE on two valence neutrons. The authors of Ref. 3 set the quantity $|B(E)|^2$ equal to the theoretical cross section calculated in Ref. 4, which was based solely on two subsequential SCE processes. The magnitude of the first amplitude was determined by requiring that $(a(E))^2$ be equal to the measured 5° pion-^{16}O DCE differential cross section at pion energy E. The quantity $\phi_a(E)-\phi_b(E)$, denoted $\Delta\phi$, was then treated as a free parameter and was determined by fitting $|A(E)+B(E)|^2$ to the measured 5° DCE differential cross section of the reaction $^{18}O(\pi^+,\pi^-)^{18}Ne$ (DIAS) at each energy. We recall that in our microscopic theory for DCE reactions the ρ^2-dependent interaction necessarily contains pion charge exchange on the valence as well as on the core nucleons. In this respect our theory incorporates explicitly the basic physical ingredients that underlie the parametrization of Ref. 3. Thus, it is not surprising that the fitting procedure of Ref. 3 has yielded, for the 5° excitation function, results similar to ours. We note, however, that the knowledge of the fitted value of $\Delta\phi$ in Ref. 3 did not lead to a quantitative prediction of the position of θ_{min} at 164 MeV. On the other hand, we are able to obtain satisfactory description of the excitation function and the angular distributions with one single set of calculations. Since, as discussed in Sec. II, the pion charge exchange on the valence neutrons can equally proceed via ρ^2-dependent irreducible two-nucleon processes which were not represented by the theoretical amplitude of Ref. 4, the fitting procedure of $\Delta\phi(E)$ based on the use of $B(E)$ inevitably mixes, therefore, effects arising from the reaction mechanism and from nuclear structure. By providing a unified treatment of the ρ^2-dependent interaction in elastic scattering and charge exchange, our theory puts a constraint on the latter. It is precisely this aspect that makes possible *quantitative* studies of nuclear structure effects such as those related to core excitations.

IV. SUMMARY AND CONCLUSIONS

The DCE reaction $^{18}O(\pi^+,\pi^-)^{18}Ne$ (DIAS) can be explained in the framework of a diffraction theory when two-nucleon processes and core excita-

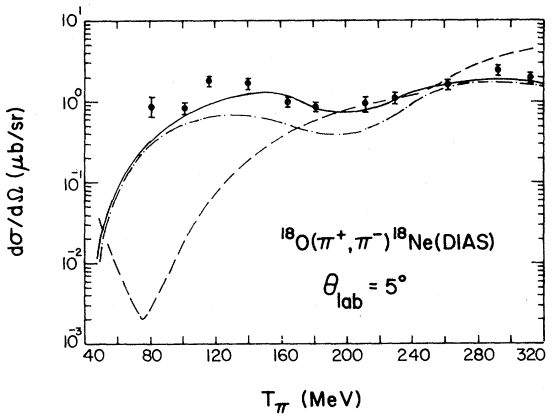

FIG. 4. Excitation functions for the reaction $^{18}O(\pi^+,\pi^-)^{18}Ne$ (DIAS). Data are from Ref. 3. Notation for curves is the same as for Fig. 1.

tion of the nucleus are included. Our study shows the significant contributions to DCE processes from the ρ^2-dependent interaction. Further, in contrast to elastic scattering, the magnitude of calculated DCE cross sections is very sensitive to the detailed composition of the nuclear wave function.

The isospin dependence of the pion-nucleus second-order interaction on the ^{18}O nucleus is determined through the scaling theory. Although the use of a scaling model is necessitated solely by the lack of systematic experimental π-^{18}O scattering data at pion energies between 50 and 300 MeV, it does provide a test of our interpretation of the main origin of the second-order pion-nucleus interaction. Our assumption that only true pion absorption contributes to the ρ^2 terms is based on our observation that in the (3,3) resonance region at least one third of the pion-nucleus reaction cross sections are due to pion absorption and that short-range correlation effects are unimportant. The success of this dynamical model in describing both elastic and charge-exchange data at many different energies provides some support for the latter. Inspection of Figs. 1 and 4 shows, in fact, no strong indication for the need of including ρ^2 terms due to short-range correlation effects. On the other hand, we have pointed out that improved large-angle differential cross section measurements at 292 MeV can aid us in obtaining more definitive information concerning such correlation effects. Clearly, measuring DCE differential cross sections at other higher energies, in particular at large angles, is equally of value.

Theoretical input to this work was fixed according to the values determined in previous studies[12,14,15]; no adjustable parameter was used. We believe that our approach represents a useful alternative to that which treats the strength of the ρ^2-dependent isoscalar, isovector, and isotensor terms as adjustable complex variables. There have been a number of discussions about the effects of ρ^2 terms on DCE reactions,[21] but in those discussions the nuclear structure effects arising from core excitations have not been elucidated. The main result of this work is the separation of the effects due to the ρ^2-dependent reaction mechanism from those due to nuclear structure. Further, our theory is able to describe, in the main, both the shapes and the magnitudes of the excitation function and the angular distributions. The present approach thus provides a useful framework in which quantitative studies of nuclear structure can be carried out. Since the DCE processes connecting the DIAS's involve transitions which are absent in electron- or proton-induced reactions, we believe that pion DCE reactions represent a valuable tool for nuclear structure studies. On the other hand, we are greatly encouraged by the results of this work to carry out microscopic calculations of second-order pion-nucleus interactions based on true pion absorption. We will also further test our model by analyzing DCE reactions on other nuclei.

This work was performed under the auspices of the U. S. Department of Energy.

APPENDIX A

We have defined scaling factors η in terms of ratios of strength functions. In this appendix, we recapitulate the notation and calculational steps employed in Ref. 8 for the determination of these quantities. We use

$$(NN)\equiv\{(nn),(np),(pn),(pp)\}$$

to denote the four physical states that can be formed with two nucleons in isospin space, where n stands for a neutron and p for a proton. The combinations (np) and (pn) are distinct since they are two orthogonal combinations of states of definite symmetry, namely,

$$|(pn)\rangle=\{|t=1\rangle+|t=0\rangle\}/\sqrt{2}$$

and

$$|(np)\rangle=\{|t=1\rangle-|t=0\rangle\}/\sqrt{2}\ ,$$

where t denotes the total isospin of the pair. One defines four basic strength functions according to

$$S(\pi^i(nn))=\langle\pi^i(nn)\,|\,S_{op}\,|\,\pi^i(nn)\rangle\ , \tag{A1}$$

$$S(\pi^i(np))=\sum_{t'=t}\langle\pi^i(np)\,|\,S_{op}\,|\,\pi^i(np)\rangle\ , \tag{A2}$$

$$S(\pi^i(pn))=\sum_{t'=t}\langle\pi^i(pn)\,|\,S_{op}\,|\,\pi^i(pn)\rangle\ , \tag{A3}$$

and

$$S(\pi^i(pp))=\langle\pi^i(pp)\,|\,S_{op}\,|\,\pi^i(pp)\rangle\ . \tag{A4}$$

In these equations, i denotes the pion charge ($i=+,0,-$) and S_{op} the interaction between π^i and two nucleons. The omission of $t'\neq t$ transitions in Eqs. (A3) and (A4) is justified by the very small contributions of these transitions to nuclear reactions, as was shown in Sec. III of Ref. 8. Further, in calculating the matrix elements of S_{op}, we have found it convenient to work with states defined by

$$|[nn]\rangle\equiv|(nn)\rangle\ ,$$

$$|[np]\rangle\equiv\sqrt{2}\,|(np)\rangle\ ,$$

and

$$|[pp]\rangle\equiv|(pp)\rangle\ .$$

It is easy to see that

$$S(\pi^i(nn))=S(\pi^i[nn]) ,$$

$$S(\pi^i(pn))=S(\pi^i(np))=S(\pi^i[np])/2 ,$$

and

$$S(\pi^i(pp))=S(\pi^i[pp]) .$$

Strength functions in this latter [ ] representation have been determined for two-nucleon processes associated with either true pion absorption or short-range correlation, and are given in Tables I and II of Ref. 8. They are functions of basic pion-nucleon scattering amplitudes which are energy dependent.

We now proceed to connect the average strength functions $\bar{S}(\pi(N_cN_c))$ and $\bar{S}(\pi^i(n_vN_c))$ in this work to the basic strength functions discussed above. Here the subscripts v and c refer, respectively, to valence and core nucleons. Similar to (N_cN_c), which stands for a group of four physical states arising from two core nucleons, the

$$(n_vN_c)\equiv\{(n_vn_c),(n_vp_c)\}$$

is an abbreviated notation for a group of two physical states associated with a valence-core nucleon pair. The strength function averaged over all four states of two core nucleons is therefore equal to

$$\bar{S}(\pi^i(N_cN_c))\equiv\tfrac{1}{4}\{S(\pi^i(n_cn_c))+S(\pi^i(n_cp_c))+S(\pi^i(p_cn_c))+S(\pi^i(p_cp_c))\} . \quad \text{(A5)}$$

Once the sum over all possible states of the pair is made explicit, the presence of the subscripts v and c is no longer necessary since, by virtue of the scaling assumption, strength functions are independent of nucleon orbits. We can therefore write

$$\bar{S}(\pi^i(N_cN_c))=\tfrac{1}{4}\{S(\pi^i(nn))+S(\pi^i(np))+S(\pi^i(pn))+S(\pi^i(pp))\} , \quad \text{(A6)}$$

$$=\tfrac{1}{4}\{S(\pi^i[nn])+S(\pi^i[np])+S(\pi^i[pp])\} . \quad \text{(A7)}$$

Similarly, we define an average strength function for the interaction between a pion and a valence-core nucleon pair by

$$\bar{S}(\pi^i(n_vN_c))\equiv\tfrac{1}{2}\{S(\pi^i(n_vn_c))+S(\pi^i(n_vp_c))\} , \quad \text{(A8)}$$

$$=\tfrac{1}{2}\{S(\pi^i(nn))+S(\pi^i(np))\} , \quad \text{(A9)}$$

$$=\tfrac{1}{2}\{S(\pi^i[nn])+\tfrac{1}{2}S(\pi^i[np])\} . \quad \text{(A10)}$$

Again, Eqs. (A7) and (A10) can be readily evaluated with the aid of Tables I and II of Ref. 8. One can easily verify that the $\bar{S}(\pi^i(N_cN_c))$ do not depend on the pion charge state, as expected, and can be simply denoted as $\bar{S}(\pi(N_cN_c))$.

APPENDIX B

In this appendix we give the formulae used for interpolating between the second-order pion-oxygen optical potential parameters determined in Ref. 12. The energy dependence of the imaginary part of the parameters is given by

$$\mathrm{Im}[F(\omega)]=\mathrm{Im}[A/(\omega-\omega_R+i\Gamma/2)] ,$$

where

$$F(\omega)=B(\omega)+k^2C(\omega)$$

or $k^2C(\omega)$. Here ω is the total pion energy, in MeV, in the c.m. frame of the pion-^{16}O system, and

$$\Gamma/2=2\gamma(kR)^3/[1+(kR)^2]$$

with k being the pion momentum, in fm^{-1}, in the c.m. frame of the pion-^{16}O system. For

$$F(\omega)=B(\omega)+k^2C(\omega) ,$$

we have $A=847.9\times10^{-4}$ fm^4 MeV, $\omega_R=285.3$ MeV, $\gamma=21.59$ MeV, and $R=1.203$ fm. For $F(\omega)=k^2C(\omega)$, the parameters are $A=849.3\times10^{-4}$ fm^4 MeV, $\omega_R=285.7$ MeV, $\gamma=23.12$ MeV, and $R=1.156$ fm.

The energy dependence of the real part of the second-order optical potential parameters is given by a dispersion relation:

$$\mathrm{Re}F(\omega)=\frac{\mathscr{P}}{\pi}\int_{M_\pi}^{\infty}\frac{\mathrm{Im}[F(\omega')]}{\omega'-\omega}d\omega'+\text{ background} .$$

Here $\mathscr{P}$ stands for the principal-value integration. Contributions to the background term are numerous.[22] They come from the bound states below the threshold as well as from contributions to $\mathrm{Im}[F(\omega')]$ in the principal-value integration at energies ω' greater than 292 MeV, the maximum available pion energy in Ref. 12. These high-energy contributions are not included in the form of $\mathrm{Im}[F(\omega)]$ given above. In this work, we do not attempt to calculate the background term from first principles; we choose instead to parametrize it with a polynomial such that it provides a smooth interpolation between the previously determined parameter values. We write, therefore,

$$\text{background}=a_0+a_1k+a_2k^2+a_3k^3+a_4k^4+a_5k^5 .$$

For

$$F(\omega)=B(\omega)+k^2C(\omega)\ ,$$

$a_0=0.0382$ fm^4, $a_1=-0.194$ fm^5, $a_2=0.377$ fm^6, $a_3=-0.342$ fm^7, $a_4=0.145$ fm^8, and $a_5=-0.232$ fm^9. For $F(\omega)=k^2C(\omega)$, we have $a_0=0.0114$ fm^4, $a_1=-0.0652$ fm^5, $a_2=0.142$ fm^6, $a_3=-0.142$ fm^7, $a_4=0.0657$ fm^8, and $a_5=-0.0110$ fm^9. We have noted that theoretical π-^{16}O elastic cross sections obtained with the interpolated parameters are almost identical to those reported in Ref. 12. The π^+-^{18}O elastic scattering cross sections based on the interpolated parameters and the scaling model are compared to available data in Figs. 2 and 3.

[1]K. K. Seth, S. Iversen, H. Nann, M. Kaletka, J. Hird, and H. A. Thiessen, Phys. Rev. Lett. 43, 1574 (1979); 45, 147(E) (1980).

[2]S. J. Greene, W. J. Braithwaite, D. B. Holtkamp, W. B. Cottingame, C. F. Moore, C. L. Morris, H. A. Thiessen, G. R. Burleson, and G. S. Blanpied, Phys. Lett. 88B, 62 (1979); J. Davis, J. Källne, J. S. McCarthy, R. C. Minehart, C. L. Morris, H. A. Thiessen, G. S. Blanpied, G. R. Burleson, K. Boyer, W. Cottingame, C. F. Moore, and C. A. Goulding, Phys. Rev. C 20, 1946 (1979).

[3]S. J. Greene, W. J. Braithwaite, D. B. Holtkamp, W. B. Cottingame, C. F. Moore, G. R. Burleson, G. S. Blanpied, A. J. Viescas, G. H. Daw, C. L. Morris, and H. A. Thiessen, Phys. Rev. C 25, 927 (1982).

[4]G. A. Miller and J. E. Spencer, Ann. Phys. (N.Y.) 100, 562 (1976).

[5]D. A. Sparrow and A. S. Rosenthal, Phys. Rev. C 18, 1753 (1978).

[6]X. Liu, Z. Wu, Z. Huang, and Y. Li, Sci. Sin. 24, 789 (1981).

[7]E. Oset, D. Strottman, and G. E. Brown, Phys. Lett. 73B, 393 (1978).

[8]L. C. Liu, Phys. Rev. C 23, 814 (1981).

[9]L. C. Liu and C. M. Shakin, Phys. Rev. C 20, 2339 (1979).

[10]Mikkel B. Johnson, Phys. Rev. C 22, 192 (1980).

[11]L. C. Liu, Phys. Rev. C 17, 1787 (1978); K. Stricker, H. McManus, and J. A. Carr, *ibid.* 19, 929 (1979).

[12]L. C. Liu and C. M. Shakin, Phys. Rev. C 19, 129 (1979).

[13]H. Überall, in *Electron Scattering From Complex Nuclei* (Academic, New York, 1971), pp. 350–366; L. C. Liu and C. M. Shakin, Phys. Rev. C 14, 1245 (1976).

[14]R. L. Lawson, F. J. D. Serduke, and T. Fortune, Phys. Rev. C 14, 1245 (1976).

[15]J. Negele, private communication.

[16]A. W. Thomas, in *Proceedings of the International Conference on Nuclear Physics,* edited by R. M. Diamond (North-Holland, New York, 1981), p. 67c.

[17]S. Iversen, H. Nann, A. Obst, K. K. Seth, N. Tanaka, C. L. Morris, H. A. Thiessen, K. Boyer, W. Cottingame, C. F. Moore, R. L. Boudrie, and D. Dehnhard, Phys. Lett. 82B, 51 (1979).

[18]S. Iversen, Ph.D. thesis, Northwestern University, 1978 (unpublished).

[19]L. C. Liu and V. Franco, Phys. Rev. C 11, 760 (1975).

[20]D. J. Herndon *et al.*, University of California Radiation Laboratory Report UCRL-20030, 1970; G. Rowe, M. Salomon, and R. Landau, Phys. Rev. C 18, 584 (1978).

[21]See, for example, Mikkel B. Johnson and E. R. Siciliano, Los Alamos National Laboratory Reports LA-UR-82-3024 and LA-UR-82-3220, 1982.

[22]T. E. O. Ericson and M. P. Locher, Nucl. Phys. A148, 1 (1970).